1. AGENCY USE ONLY (Leave blank)	2. REPORT DATE	3. REPORT TYPE AND DATES COVERED
		Final Report 15 Jul 92 – 14 Jul 93

4. TITLE AND SUBTITLE	5. FUNDING NUMBERS
YBCO JOSEPHSON JUNCTION ARRAYS	F49620-92-C-0048

6. AUTHOR(S)

Dr Randy Simon

7. PERFORMING ORGANIZATION NAME(S) AND ADDRESS(ES)	8. PERFORMING ORGANIZATION REPORT NUMBER
Conductus 969 West Maude Avenue Sunnyvale CA 94086	AFOSR-TR- 94 0075

9. SPONSORING MONITORING AGENCY NAME(S) AND ADDRESS(ES)	10. SPONSORING MONITORING AGENCY REPORT NUMBER
AFOSR/NE 110 Duncan Avenue Ste B115 Bolling AFB DC 20332-0001	1601/07

11. SUPPLEMENTARY NOTES

12a. DISTRIBUTION AVAILABILITY STATEMENT

UNLIMITED

13. ABSTRACT (Maximum 200 words)

Josephson junction arrays have long been suggested as efficient, tunable sources for upper microwave and mm-wave frequencies. Based on the fundamental properties of the junction and the ability to combine the power output of many junctions using an array, the circuit concept is quite promising. The challenge is to phase lock the junctions so that power adds coherently and a number of demonstrations with Nb junction arrays have been performed doing this. This program was intended to begin using YBCO junction arrays to demonstrate source potential at 77K. Edge junctions have been used in arrays with up to 60000 junctions and the ability to couple power off-chip has been demonstrated directly for frequencies of at least 70-160 GHz. Power outputs have approached 1 uW (in relatively narrow bands) and tunability has exceeded 20 GHz. Some novel array architectures have been built, including one with improved linewidth per unit junction, and new techniques developed for extracting junction statistics from array spectra. These techniques are used as feedback for process optimizations now in progress.

DTIC QUALITY INSPECTED 1

14. SUBJECT TERMS			15. NUMBER OF PAGES
			27
			16. PRICE CODE

17. SECURITY CLASSIFICATION OF REPORT	18. SECURITY CLASSIFICATION OF THIS PAGE	19. SECURITY CLASSIFICATION OF ABSTRACT	20. LIMITATION OF ABSTRACT
UNCLASS	UNCLASS	UNCLASS	UL

NSN 7540-01-280-5500

AFOSR-TR· 94 0075

FINAL REPORT

CONTRACT F49620-92-C-0048

YBCO JOSEPHSON JUNCTION ARRAYS

EXECUTIVE SUMMARY

Josephson junction arrays have long been suggested as efficient, tunable sources for upper
microwave and mm-wave frequencies. Based on the fundamental properties of the junction and
the ability to combine the power output of many junctions using an array, the circuit concept is
quite promising. The challenge is to phase lock the junctions so that power adds coherently and
a number of demonstrations with Nb junction arrays have been performed doing this. This
program was intended to begin using YBCO junction arrays to demonstrate source potential at
77K. Edge junctions have been used in arrays with up to 60000 junctions and the ability to
couple power off-chip has been demonstrated directly for frequencies of at least 70-160 GHz.
Power outputs have approached 1 μW (in relatively narrow bands) and tunability has exceeded
20 GHz. Some novel array architectures have been built, including one with improved linewidth
per unit junction, and new techniques developed for extracting junction statistics from array
spectra. These techniques are used as feedback for process optimizations now in progress.

1. Background and objectives

The object of this program was to determine the best approach and to construct one and two-dimensional arrays of YBCO Josephson junctions with the purpose of making oscillators. While originally bi-epitaxial junctions were envisioned as the junction technology of choice (one of the best available at the time the proposal was written), better technologies surfaced in the interim. Thus while the goals and objectives do not change on the surface, the underlying technology may have shifted somewhat from that originally planned. The program objectives (following option 1) are

A. Design and procure diagnostic and circuit masks to test junctions, passive structures and simple 1-D and 2D arrays. Make chips and test using these mask sets

B. Design and procure a second generation mask set using tighter dimensional diagnostics and the most promising array structures. Fabricate and test chips using this second generation of masks.

Overall, the goal of the program is to establish some promising array structures for exploitation and development into possible applications in follow on programs. The theoretical advantages of Josephson arrays as sources, if they can be achieved, would make these attractive micro-/mm-wave oscillators for commercial and military applications.

2 Status of research effort

Much work has been done in the field of LTS Josephson arrays, e.g. [1]-[3]. If such oscillators could be adapted to YBCO for operation near 77K, a number of additional practical advantages could be achieved.

2.1 Junctions

At the time of proposal, the primary junction being investigated at Conductus (and one of the better performing junctions in the community) was the bi-epitaxial structure [4]. In this junction, discussed extensively in the proposal, a seed layer is used to force a 45 degree rotation in the

FINAL REPORT

CONTRACT F49620-92-C-0048

YBCO JOSEPHSON JUNCTION ARRAYS

<u>EXECUTIVE SUMMARY</u>

Josephson junction arrays have long been suggested as efficient, tunable sources for upper microwave and mm-wave frequencies. Based on the fundamental properties of the junction and the ability to combine the power output of many junctions using an array, the circuit concept is quite promising. The challenge is to phase lock the junctions so that power adds coherently and a number of demonstrations with Nb junction arrays have been performed doing this. This program was intended to begin using YBCO junction arrays to demonstrate source potential at 77K. Edge junctions have been used in arrays with up to 60000 junctions and the ability to couple power off-chip has been demonstrated directly for frequencies of at least 70-160 GHz. Power outputs have approached 1 μW (in relatively narrow bands) and tunability has exceeded 20 GHz. Some novel array architectures have been built, including one with improved linewidth per unit junction, and new techniques developed for extracting junction statistics from array spectra. These techniques are used as feedback for process optimizations now in progress.

1. Background and objectives

The object of this program was to determine the best approach and to construct one and two-dimensional arrays of YBCO Josephson junctions with the purpose of making oscillators. While originally bi-epitaxial junctions were envisioned as the junction technology of choice (one of the best available at the time the proposal was written), better technologies surfaced in the interim. Thus while the goals and objectives do not change on the surface, the underlying technology may have shifted somewhat from that originally planned. The program objectives (following option 1) are

A. Design and procure diagnostic and circuit masks to test junctions, passive structures and simple 1-D and 2D arrays. Make chips and test using these mask sets

B. Design and procure a second generation mask set using tighter dimensional diagnostics and the most promising array structures. Fabricate and test chips using this second generation of masks.

Overall, the goal of the program is to establish some promising array structures for exploitation and development into possible applications in follow on programs. The theoretical advantages of Josephson arrays as sources, if they can be achieved, would make these attractive micro-/mm-wave oscillators for commercial and military applications.

2 Status of research effort

Much work has been done in the field of LTS Josephson arrays, e.g. [1]-[3]. If such oscillators could be adapted to YBCO for operation near 77K, a number of additional practical advantages could be achieved.

2.1 Junctions

At the time of proposal, the primary junction being investigated at Conductus (and one of the better performing junctions in the community) was the bi-epitaxial structure [4]. In this junction, discussed extensively in the proposal, a seed layer is used to force a 45 degree rotation in the

plane of grain growth for 1/2 of the junction. The resulting high-angle grain boundary forms the junction. These junctions have useful absolute parameters (and have been used in commercial products) but have very large spreads on a wafer. Based on array simulations, the spreads are sufficiently large that enough phase locking in an array to generate measurable radiation seems unlikely.

Since the proposal stage, however, numerous other junction technologies have been developed. One internal technology is based on SNS junctions [5]. This junction structure uses a $CaRuO_3$ or other normal metal layer separating two $YBa_2Cu_3O_7$ layers in an edge geometry[4] as suggested by Fig. 1a. $CaRuO_3$ is desirable as a barrier layer for a number of reasons. It is a cubic perovskite with a lattice parameter of 3.85 Å, which falls between the *a* and *b* lattice parameters of $YBa_2Cu_3O_7$, it is metallic, and can be grown in conditions compatible with $YBa_2Cu_3O_7$. Also, $CaRuO_3$ is chemically compatible with $YBa_2Cu_3O_7$ and its conductivity does not appear to be strongly dependent on doping or oxygen concentration. Both the superconducting and the barrier films are laser ablated. An edge geometry was used to keep the critical currents reasonable since the barrier conductivity is quite high. The first $YBa_2Cu_3O_7$ layer and the $SrTiO_3$ layer are deposited first and then patterned with ion milling (to help form the edge). The $CaRuO_3$ and second $YBa_2Cu_3O_7$ layers are then deposited before the next patterning step. Passivation and normal metal contact layers are then applied and patterned.
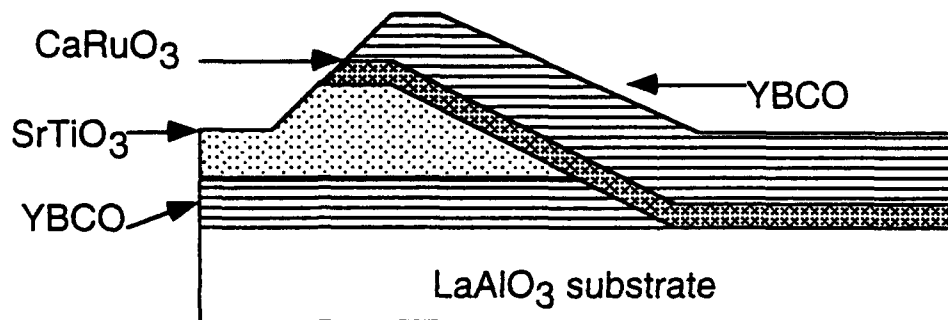

Figure 1. Structure of the SNS edge junction.

For a 4 μm wide junction, critical currents are typically in the range of 100 μA at 77K with a corresponding normal state resistance of about 1 Ω. Spreads are considerably better. Three sigma values of ±40% and better have been measured (dependent somewhat on the exact barrier being used) which, based on simulation, should be sufficient for array phase locking and detectable radiation.

2.2 Diagnostics and array types measured

A variety of diagnostic test structures were included on the test masks to check the status of the process. This was done in conjunction with other programs and the results were generally quite satisfactory. While there are many circuit and process parameters of general interest, not all will be discussed here. The upper and lower YBCO levels never pass over each other except at a junction and at that point, the edge junction will dominate any leakage through the $SrTiO_3$, thus the integrity of that dielectric will not be a concern here. The integrity of the dielectric between a normal metal wiring level and the YBCO is of potential concern but 400 μm^2 capacitors showed resistances > 10 kΩ. Based on the junction impedances discussed above, this is not a concern.

The wiring interconnect integrity was found not to be a problem, even when going over 200 nm thick structures on the lower level (less than a 20% degradation in conductivity). Contact resistance is primarily an issue in the sense of the bias pads and any interconnect pads. The smallest such structures envisioned in this work is 100 μm x 100 μm. The contact resistance was found to be less than 10 mΩ for such pads which, based on array impedances, should not represent a problem.

The only remaining diagnostic is the junction proper. A large number of test chips have been made to make preliminary evaluations of uniformity and the absolute parameters possible. These have generally been done on dedicated 1/4" test chips designed for compatibility with a variable temperature probe. A sample IV curve is shown below.
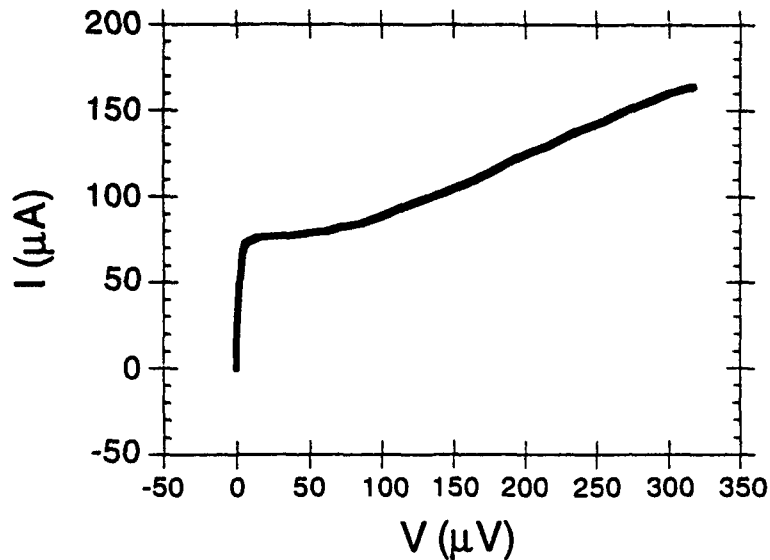
Figure 2. IV curve of an SNS junction. The steps shown here are the result of digitization rather than being physical.

Both 1-D and 2-D arrays were made. The generic structures are shown in Fig. 3. One dimensional arrays are, of course, simpler but are more susceptible to trouble from junction non-uniformities. Obviously an open junction will doom a 1-D array but phase locking is also more difficult. The 2-D arrays are much more capable of achieving a phase lock with presently practical parameter spreads but are more subject to chaos and vortex nucleation.
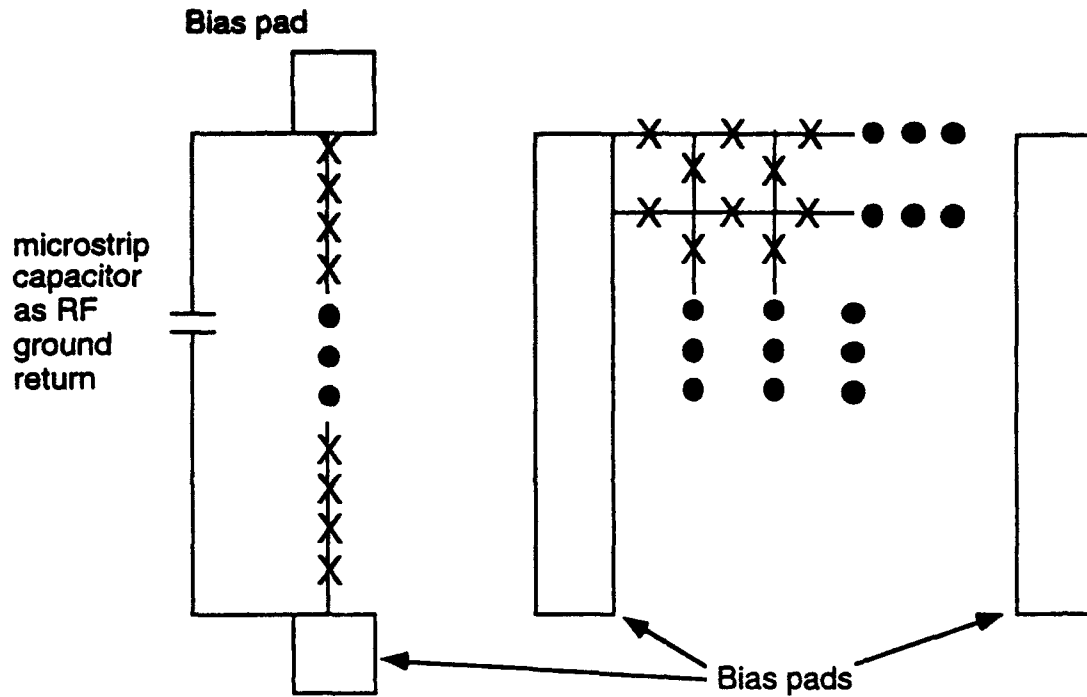
Figure 3. Typical 1-D and 2-D array structures that were built and tested.

The topology of the actual 2-D array structure is shown in Fig. 4. Four μm-wide junctions are used and no particular wiring levels are needed. A simple set of normal metal contacts are provided for bias and IV curve measurement.
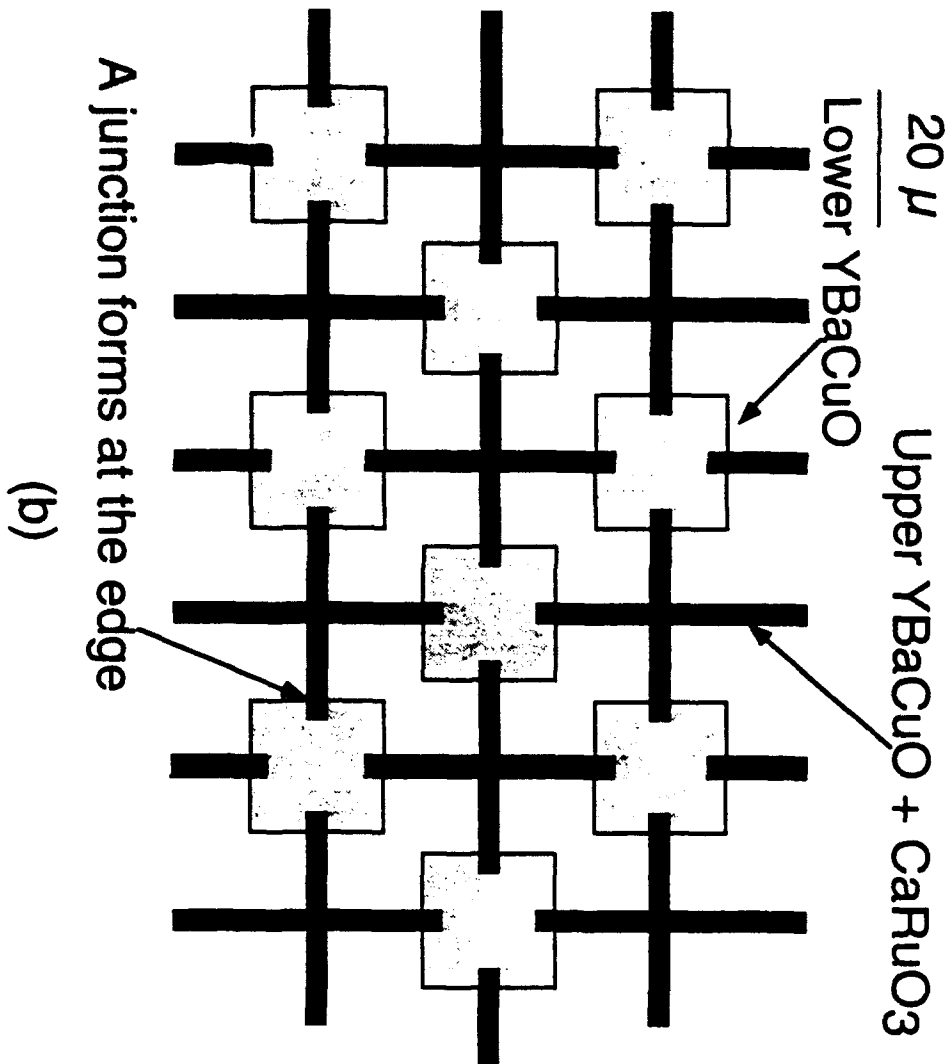
Figure 4. Physical structure of a 2-D SNS array.

2.3 Results: IV curves, radiation measurements and resonator links

Both isolated arrays and those embedded in log-periodic spiral antennas [6] have been used. In the latter case, the array is electromagnetically, a lumped element at the frequencies of interest and is placed at the apex of the antenna. The antennas are monolithic (fabricated in the lower $YBa_2Cu_3O_7$ film) designed for operation in the range 60-250 GHz. Based on present circuit time constants, it is believed the arrays can operate at least up to the 250 GHz antenna upper bound. The L/R circuit time constants (arising from array interconnect plus Josephson inductances and junction resistance) would have limited the bandwidth to something under 500

GHz anyway so the antennas do not represent a major design problem. For some measurements, the isolated arrays were used as half of a quasi-optical confocal resonator [7] (the other half being a spherical aluminum mirror). By making the array an integral part of such a high quality factor resonator, it is easier to lock the array to a particular frequency to decrease linewidths. The dominant transverse electromagnetic (TEM) resonator modes are characterized by both E and H fields tangential to the array and linearly polarized. Coupling to the junctions in this rectilinear array is therefore relatively easy. Since reasonable power levels could be coupled out of the resonant structure with small linewidths, it may be a useful arrangement for some applications.

Three specific topologies will be discussed here. Type A is a square array without an antenna consisting of 361 participating junctions (19 parallel columns of 19 junctions each) and 361 cross-junctions. Type B is also a square array without an antenna but consists of 28900 participating junctions (170 columns of 170 junctions each) and 28900 cross-junctions. Type C is a rectangular array of 352 participating junctions (11 columns of 32 junctions each) and 352 cross junctions embedded in a log-periodic spiral antenna. The array critical current will be approximately the number of columns multiplied by the junction critical current.

An IV curve for an array of type A is shown in Fig. 5 for the bare array and for the same array locked to a confocal resonator. The composite critical current and normal state resistance are as expected for this array type based on a junction critical current of 40-45 μA and an R_n of about 1 Ω (measured from witness junctions fabricated during the same process run). The basic IV curve is quite clean and RSJ-like, suggesting that the inhomogeneities in the array parameters are reasonable and there are not large concentrations of non-functional junctions. When the array is positioned to form one end of a confocal resonator, the phase locking to the resonant mode becomes obvious. The strongest steps correspond to dominant TEM_{00n} modes discussed earlier (the steps at 0.23, 0.29 and 0.35 mV) into which this array can most easily launch. Six of these arrays were measured with similar IV curves (with and without the confocal resonator) and critical currents ranged from 700-800 μA. A type B array was also measured with a qualitatively similar result in that the IV curve was clean/RSJ-like and steps were visible at points corresponding to resonant modes. The steps were slightly more difficult to see with this array since they were positioned closer to the critical current. The total critical current in that case was about 6.8 mA with a composite normal state resistance of about 1.2 Ω.

The spectrum for an array embedded in a log-periodic spiral antenna (type C) was measured near 97 GHz and showed a peak power level of about 2 nW in a 3 MHz bandwidth measured at the

receiver (broadband power was about 0.3 μW, over 1 pW/Hz$^{0.5}$ narrowband). The power from the antenna was coupled with a 25 dB gain horn antenna feeding a calibrated harmonic mixer/spectrum analyzer combination.   At this temperature, one would expect a linewidth of order 10 MHz if all of the junctions were phase locked and there were negligible parameter variations [2],[9]. Since there significant parameter variations, it is not surprising that this theoretical linewidth was not obtained [1]. Nonetheless the linewidth is considerably narrower than that from a single junction or from a small array of junctions. The array was also found to be bias tunable over most of the bandwidth of the receiving system (90-160 GHz) with amplitude variations of less than 5 dB. Locking to a high Q resonator such as the confocal resonator produced very narrow oscillations (of order 3 MHz centered at 96 GHz) which may be of use in a number of applications.

The spectrum of an isolated type B array, placed 1 cm from the horn entrance, was measured with a linewidth of approximately 10 MHz (the theoretical value assuming no parameter variations is about 180 kHz) centered at 110 GHz as shown in Fig. 6. The spectrum shown in Fig. 6 is corrected for the minor frequency dependence of the horn gain. It is expected that the linewidth will scale inversely as the number of participating junctions if the parameter spreads are approximately constant [2]. If one were to scale the measured linewidth of the type C array to be equivalent to the size of the type B array, one gets about 8 MHz which is quite close to the measured value. Since this array is much larger, it is expected that there were larger parameter spreads from film variations alone. On the subject of power levels, the coupling on this type B array is much poorer because of the lack of an antenna. Even with this problem, the spectral peak was about 1 μW in a 3 MHz bandwidth measured at the receiver (nearly 1 nW/Hz$^{0.5}$).

We have demonstrated likely coherent radiation from HTS Josephson array sources in the 90-160 GHz range with up to nearly 60000 junctions. Over 1 μW has been coupled out (and in some cases that was weakly coupled) when using broadband antennas on chip and tunability over fairly wide bandwidths (tens of GHz) has been demonstrated. Resonator coupling has also been used to demonstrate power extraction with narrow linewidths.
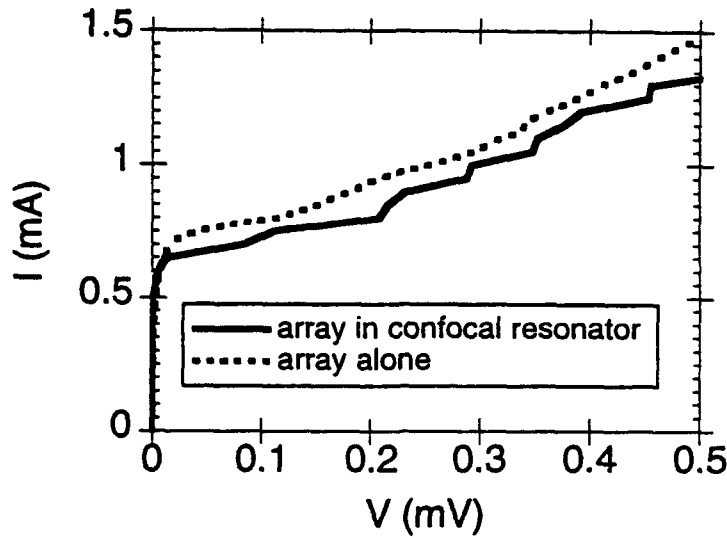
Figure 5. An IV curve of a 2D array with a total of 722 junctions. One curve is for the bare array and shows RSJ-like behavior and a critical current consistent with the average for the process run. The overlay shows the IV curve when the array is placed in a confocal resonator. Locking to various confocal resonator modes is obvious.
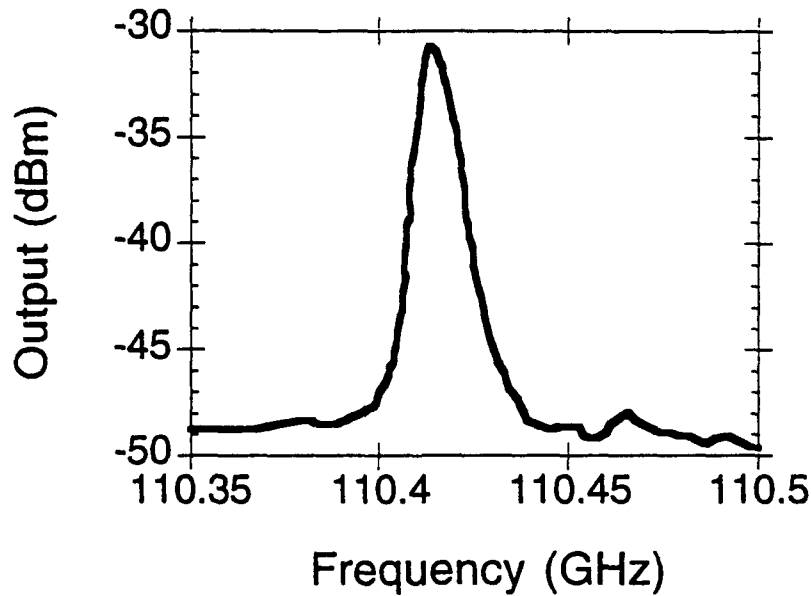
Figure 6. A spectrum of a 2D array showing nearly 1 μW (3 MHz bandwidth) output power at 110 GHz. The signal was measured with a conventional 25 dB gain horn antenna placed 1 cm from the array.

Other topologies, more speculative in nature, have also been tried. The topology of Fig 7 is a 2D array with 8 extra interlink junctions added per unit cell (a 2x increase in junction density with no increase in process complexity). By adding additional paths for current redirection, the effects of paramater variations can be further minimized. Since the effective system inductance is also being reduced, some of the voretx nucleation problems can also be reduced (although the simulations at present do not address this issue). According to simulations, this results in about a 2x increase in phase locking probability, a 4x increase in power output and factor of 2.5 reduction in linewidth. These calculations all assume typical SNS junction parameters and typical layout rules.
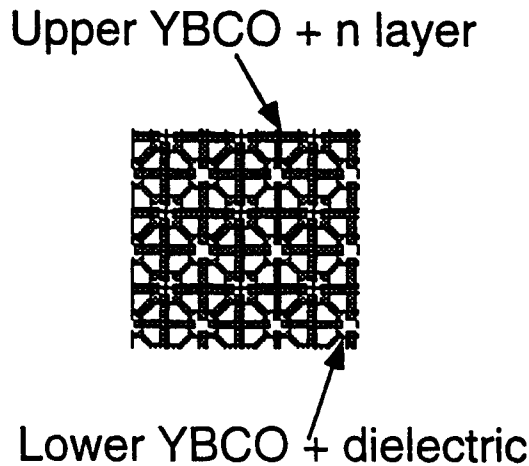
Upper YBCO + n layer

Lower YBCO + dielectric

Figure 7. Modified 2-D array topology allowing easier current redirection and a lessening of the effects of parameter spread.

Many of these results expected from simulation have been confirmed by experiment. A series of test arrays have been fabricated using standard 2D arrays and the two invented topologies of Fig. 2. The standard 2D array consisted of 342 junctions in the flow columns plus an additional 342 cross junctions. The type Q topology was fabricated with a total of 1368 junctions and type 2b arrays with 2052 junctions. In all cases, the nominal junction critical current was 40 μA and the normal state resistance was about 2 Ω. All tests were conducted at 77K. Five ordinary 2D arrays and 3 type A arrays were found to be functional in this particular run. The table below shows the output powers and fractional linewidths observed (operating at $\approx$150 GHz). The trends confirm the simulation to a large degree and illustrate the advantages of the new topologies in output power and linewidth above and beyond what would be expected just from junction count (which would predict about a 1.5x linewidth reduction and 2x power improvement.

ARRAY TYPE and #	POWER OUTPUT (dBm)	FRACT. LINEWIDTH
2D-1	-32	0.0020
2D-2	-35	0.0024
2D-3	-40	0.0050
2D-4	-32	0.0031
2D-5	-33	0.0038
TYPE Q-1	-25	0.0010
TYPE Q-2	-27	0.0012
TYPE Q-3	-27	0.0009

2.4 Spectral analysis and extracted margins

One interesting application of array spectra is the extraction of statistical information about the junctions. Since an increase in average spread correlates very well with an increased linewidth, it may be possible to back calculate from the measured spectra an estimate of the junction statistics [3]

We start by assuming that the junction parameters are normally distributed and independent. This is dangerous for the smaller arrays (since many variations can be traced to larger scale process deviations) but satisfactory comparisons with DC data have been obtained so far as will be shown. Then, for a given array topology and bias conditions, there are four unknowns in the system: mean critical current ($<I_c>$) , standard deviation of critical current (σI_c), mean normal state resistance ($<R_n>$), and standard deviation of normal state resistance (σR_n). From the known bias data and array geometry, it is possible to extract reasonable estimates of $<I_c>$ and $<R_n>$. The fitting routines will then be used to extract the remaining two parameters from the normalized spectrum. The spreads σI_c and σR_n both affect the shape of the spectrum but the effect of spreads in critical current are particularly dramatic [2]. The accuracy of the extraction of σI_c is therefore expected to be better than that for σR_n as will be discussed below.

The measured spectra are fit (via a Levenberg-Marquardt algorithm [8]) to that computed from a self-consistent simulation of the structure illustrated in Fig. 4. As discussed by several groups [2], the two-dimensional structures are considerably more forgiving to defects and deviations because of the myriad of alternate current paths available. The analysis begins with Kirchoff's law applied at each node of the array. The junctions are assumed to be RSJ-like at least in the sense that the low-temperature IV curve nearly fits the theory and the usual voltage-phase relation holds. Thermal noise is modeled by a modification of the analysis by Ambegaokar and

Halperin [9], although it is believed that this will overestimate the broadening for some of the junction technologies since the current-phase relationships are not perfectly sinusoidal. Each junction is assumed to be coupled to an external impedance (a ground plane is always assumed) which is composed of a radiation resistance and some near-field impedance. While the former is important for computing the loading and output power coupling, the latter represents an additional coupling mechanism between the junctions in the array. These contributions are estimated from finite element techniques but one can see they arise from surface wave mode coupling, microstrip patch coupling and dielectric reflection [10]. Based on work with arrays of FETs and diodes [11]-[12] and due to the high dielectric constants involved, we will assume that the reactive part of this coupling impedance is predominantly capacitive. Loop inductance was neglected since for the arrays geometries analyzed here, each loop had less than about 1 pH of inductance. The individual loop LI_c product was always less than $0.05\Phi_0$ so flux quantization was neglected. Quantization in multiple loops is physically possible [2] and, in general, should be considered but it is less likely in the present geometries. The phase at each node ϕ_j is the state variable [2-3]. The equation for node j is then

$$\sum_{i=1}^{N_j} \left[I_{c,i,j} \sin(\phi_i - \phi_j) + \frac{\hbar}{2eR_{i,j}} \frac{\partial(\phi_i - \phi_j)}{\partial t} \right]$$
$$+ \sum_{k=1}^{N} \frac{\hbar}{2e} \left[B_{k,j} \frac{\partial(\phi_k - \phi_j)}{\partial t} + C_{k,j} \frac{\partial^2(\phi_k - \phi_j)}{\partial t^2} \right] = I_{ext,j}$$

where $I_{c,i,j}$ and $R_{i,j}$ describe the junction connecting nodes i and j, N_j is the number of nearest neighbors to node j and N is the total number of nodes. The second summation represents the coupling impedances discussed above (first term resistive, second term capacitive). For interior nodes, $N_j=4$ for the standard 2D structure shown in Fig. 4. Variations on this present structure allow values up to $N_j=16$ (all data and further analysis refers only to the standard 2D structure). For junctions on the edge of the array in the standard structure, N_j is 3.

The B_{kj} and C_{kj} terms describe the coupling between junctions (multi-junction interactions are not considered explicitly) through surface modes and the near fields (B_{kk} and $C_{kk} =0$). These values are *numerically* estimated through finite element simulations based on a pair of junctions in the environment of the circuit: on the $LaAlO_3$ or YSZ substrate with ground plane. All of the parameters will not be shown here for space reasons but for the arrays analyzed in this paper, the nearest neighbor B_{kj} values were always below 0.2 in absolute value (much smaller in some cases, see the arrays section) and the nearest neighbor C_{kj} values were below 10^{-12}. The C_{kj}

values fall off super-linearly with node separation but the B_{kj} interactions fall off sub linearly (representing the surface mode components). While it appears from the measurements and simulations that the nearest neighbor interactions dominate, the effect of the ground plane cannot be neglected because of the substantial effects on impedance, the addition of capacitance and the promotion of surface modes. Normal metal ground planes were used experimentally but perfect conductors were assumed for the calculations. Clearly both B and C values will increase as the substrate gets thinner or as the dielectric constant increases. As the array packing increases or electrode width increases, the direct coupling parameters C increase but B values do not change much. If the metallization occupies a very large fraction of the surface the B parameters do increase and their spatial dependence flattens out (a parallel plat mode is more likely). These dependencies combine to create different B and C parameters for the various arrays.

$I_{ext,j}$ is the external current applied to node j and is zero for all interior and top/bottom nodes. For nodes that are biased, $I_{ext,j}$ is equal to the bias current per row multiplied by ± 1 depending on the exact bias arrangement used. For these experiments, the bias is applied uniformly from the side bias pads although many other possibilities are of interest [13].

The usual approach is to formulate the phase derivatives as a function of the phase state variable Φ and solve the differential equation system conventionally in time. That is, we desire a system of the form

$$
\begin{bmatrix}
\dfrac{\partial \phi_1}{\partial t} \\
\bullet \\
\bullet \\
\bullet \\
\dfrac{\partial \phi_{2N}}{\partial t}
\end{bmatrix}
=
\begin{bmatrix}
f_1(\Phi) \\
\bullet \\
\bullet \\
\bullet \\
f_{2N}(\Phi)
\end{bmatrix}
$$

but as presently formatted, the system is described by

$$
[A]
\begin{bmatrix}
\dfrac{\partial \phi_1}{\partial t} \\
\bullet \\
\bullet \\
\bullet \\
\dfrac{\partial \phi_{2N}}{\partial t}
\end{bmatrix}
=
\begin{bmatrix}
g_1(\Phi) \\
\bullet \\
\bullet \\
\bullet \\
g_{2N}(\Phi)
\end{bmatrix}
$$

where Φ represents all of the nodes phases $\phi_1, ..., \phi_{N;}$, f_i and g_i are functions of the node phases, the junction parameters, the stimulus and the topology. The state variable $\phi_{N+1}, ..., \phi_{2N}$ are dummy variables for the first derivatives of the phases (following the standard approach of solving a second order system by converting it to a larger first order system). To understand the terms in this system, consider node p which initially we assume to not be on an edge. By looking at the first equation, the dominant elements of A in the pth row are (Q=number of junctions per row of the array):

$$a_{p,p+1} = \frac{1}{R_{p,p+1}} + B_{p,p+1}$$

$$a_{p,p-1} = \frac{1}{R_{p,p-1}} + B_{p,p-1}$$

$$a_{p,p+Q} = \frac{1}{R_{p,p+Q}} + B_{p,p+Q}$$

$$a_{p,p-Q} = \frac{1}{R_{p,p-Q}} + B_{p,p-Q}$$

$$a_{p,p} = -\frac{1}{R_{n,p,p-Q}} - \frac{1}{R_{n,p,p+Q}} - \frac{1}{R_{n,p,p-1}} - \frac{1}{R_{n,p,p+1}} - B_{p,p+1} - B_{p,p-1} - B_{p,p+Q} - B_{p,p-Q} - C_{p,p+N+1}$$

$$-C_{p,p+N-1} - C_{p,p+N+Q} - C_{p,p+N-Q}$$

The other terms in the row are straightforward to derive from Eq. 1. The corresponding $g_p(\Phi)$ is given by

$$g_p(\Phi) = -\frac{2e}{\hbar}\left[\begin{array}{l} I_{c,p,p+1}\sin(\phi_{p+1} - \phi_p) + I_{c,p,p-1}\sin(\phi_{p-1} - \phi_p) \\ +I_{c,p,p+Q}\sin(\phi_{p+Q} - \phi_p) + I_{c,p,p-Q}\sin(\phi_{p-Q} - \phi_p) \end{array}\right]$$

For nodes on the right edge of the matrix, $a_{p,p-1}=0$ and the second term in g_p is replaced by $-I_{ext,p}$. For nodes on the left edge, $a_{p,p+1}=0$ and the first term in g_p is replaced by $-I_{ext,p}$. For nodes on the top edge, $a_{p,p-Q}=0$ and the fourth term in g_p is replaced by 0. For nodes on the bottom edge, $a_{p,p+Q}=0$ and the third term in g_p is replaced by 0. The terms for the corner nodes are obvious extensions of this reasoning. To clean up the details on the dummy variables, $g_{N+k}=\phi_k$ and $a_{N+k,l}=\delta_{kl}$ for k running from 1 to N.

Since the matrix A is dependent only on the array topology and the effective junction resistances, it can be pre-computed and inverted before the differential equation is solved. Depending on the coupling coefficients B_{jk} and C_{jk}, the matrix A is not particularly sparse and general routines must be used. If the ground plane is far away (not an advisable situation based on resultant poor

power coupling to the measurement apparatus), sparse matrix techniques can sometimes be employed.

During the differential equation solution period, the phase derivative vector can then be quickly computed based on present phase values. This is computationally more efficient and far more robust than relying on previous values of the phase derivative. The differential equation is solved using a Bulisch-Stoer method [8] with adaptive step-size control. Since the solution to this problem is relatively smooth , this is a computationally efficient approach. Because this is a time domain calculation, the result itself is not of prime interest but rather the power spectrum is. The computation is continued for approximately 1000 cycles after periodicity in the terminal waveform is established. The power spectrum of the resulting waveform is then computed using fast Fourier techniques and a Welch window [8]. The resulting spectrum is normalized and compared to the measured spectrum in an RMS sense over a frequency range of 5 times the linewidth of the measured signal. The measured spectrum was corrected for the frequency dependence of the receiving measurement system before this process. This routine is repeated 10-20 times in a Monte Carlo fashion. Because of the averaging nature of the array, many Monte Carlo iterations were not needed unless a particularly bizarre distribution was obtained (e.g., a statistical freak such as a cluster of dead junctions). The average of these error functions was fed back as the error for the fitting routine.

Arrays with 200-2500 junctions have been simulated using this technique although the more common case has approximately 400 junctions which were most often fabricated. On a computer based on a Motorola 68040 microprocessor operating at 33 MHz, a fit for a 400-junction array took approximately 2 hours while for the 2500 junction arrays, the fit took approximately 3 days. The precision requested for these benchmarks was about 10^{-4} on the parameter spreads and the accuracy is expected to be within 10% on σI_c. Because of the weaker dependence of spectral shape on σR_n, the accuracy is expected to be only about 20%. Changes in R_n most clearly affect the tails of the spectrum making the extraction of that parameter even more difficult if the coupled signal is weak. Also, it is assumed that $\sigma R_n \approx \sigma R$ since the junction resistance does dominate the interaction between nearest neighbors. It must be emphasized that the above numbers are errors on the spreads and not spreads themselves.

Type D arrays discussed in this paper are composed of SNS YBaCuO junctions [5] and consisted of 19 rows and 19 columns for a total of 722 junctions. All arrays were measured at 77K and a representative spectrum along with the fit are shown in Fig. 8. The spectra were measured using a horn antenna coupled to a heterodyne receiver operating over the range 90-160 GHz with a

minimum noise floor of approximately -80 dBm. Power was coupled with 20 dB gain rectangular waveguide horns (W or D band) placed 4 to 10 cm above the array (position adjusted for maximum power, spectra observed not to change in shape). The angular orientation of the horn was adjusted in all cases for maximum power (generally obtained when the short wall was aligned with the bias current direction). The receiver (a spectrum analyzer harmonic mixer) was calibrated and the accuracy of the power levels is approximately ±2 dB. The orientations were adjusted for maximum power since the high dielectric constant of the substrate impeded coupling somewhat. This coupling was not estimated for these experiments, absolute power entering the horn was measured directly, since the spectral shape was of more interest.

These spectra have been corrected for the frequency dependence (before the normalization to a peak value of 1) of the receive antenna and down-conversion circuitry which were measured independently using a commercial broadband source. The interpretation of the absolute power levels of some of these arrays are discussed elsewhere [1] but here they tended to be on the order of tens to hundreds of nW for all of the arrays (varying sizes and none with antennas on chip). These power levels are affected by the non-uniformities as well as the coupling structure used in the given implementation and hence should not be compared directly. The power levels are, however, consistent with DC power levels (efficiency of a few %) and DC IV curve step-sizes.
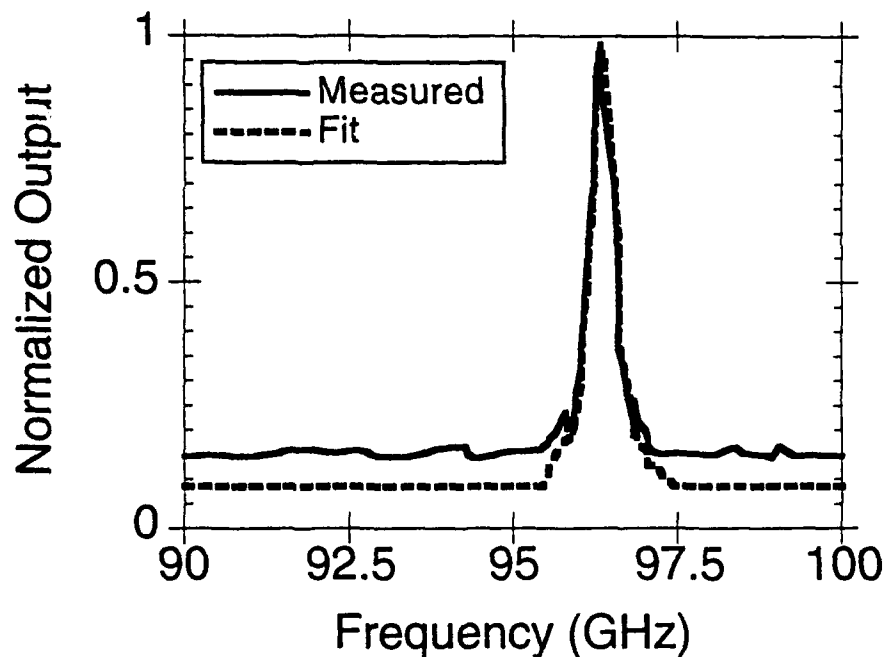

Figure 8. Measured and fit spectra of an SNS array. The baseline is not fit in this process and is somewhat arbitrary.

The statistics for the array extracted from the spectra are shown below along with DC parameters measured from a chip of junctions produced at approximately the same time. There was a difference in the barrier thickness used so the parameters are not that close absolutely but the fractional spreads are quite close.

Parameter	SNS
$\langle I_c \rangle$ DC	105 μA
$\langle I_c \rangle$ arrays	50 μA
σI_c DC	15 μA
σI_c arrays	7 μA
$\langle R_n \rangle$ DC	0.75 Ω
$\langle R_n \rangle$ arrays	1.2 Ω
σR_n DC	0.08 Ω
σR_n arrays	0.12 Ω

These results do suggest the power of array-based data extraction. Very few measurements are need and they are very fast but a wealth of data for large arrays can be extracted. Based on comparisons with many arrays, the data seems quite valid and the intrachip statistics are over large enough numbers to be extremely useful. Such measures are currently in use at Conductus for process optimization feedback.

2.5 References

[1] M. Octavio, C. B. Whan, and C. J. Lobb, Appl. Phys. Lett. **60**, 766 (1992)

[2] S. P. Benz and C. J. Burroughs, Appl. Phys. Lett. **58**, 2162 (1991)

[3] K. Wan, B. Bi, A. K. Jain, L. A. Fetter, S. Han, W. H. Mallison, and J. E. Lukens, IEEE Trans. on Mag. **27**, 3339 (1991)

[4] K. Char, M. S. Colclough, S. M. Garrison, N. Newman, and G. Zaharchuk, Appl. Phys. Lett. **59**, 733 (1991).

[5] K. Char, M. S. Colclough, T. H. Geballe, and K. E. Myers, Appl. Phys. Lett. **62**, 197 (1993).

[6] W. Stutzman and G. Thiele, <u>Antenna theory and design</u> (Wiley, New York, 1981), Ch. 6.

[7] G. D. Boyd and J. P. Gordon, Bell Sys. Tech. Jour. **40**, 489 (1961).

[8] W. H. Press, B. P. Flannery, S. A. Teukolsky and W. T. Vetterling, <u>Numerical recipes: the art of scientific computing</u> (Cambridge University Press, New York, 1990).

[9] V. Ambegaokar and B. J. Halperin, Phys. Rev. Lett. **22**, pp. 1364-1366, Jun. 1969.

[10] R. F. Harrington, <u>Time-harmonic electromagnetic fields</u> (McGraw-Hill, New York, 1961).

[11] R. A. York and R. C. Compton, 1990 IEEE Ap-S Int. Symp. Dig., Dallas, TX, May 1990, pp. 1146-1149.

[12] Z. B. Popovic, R. M. Weikle, M. Kim, and D. B. Rutledge, IEEE Trans. Micr. Theory and Tech. **39**, pp. 193-200, Feb. 1991.

[13] J. U. Free, S. P. Benz, M. S. Rzchowski, M. Tinkham, C. J. Lobb, and M. Octavio, Phys. Rev. B **41**, pp. 7267-7269, Sept. 1990

[14] J. S. Martens, A. Pance, K. Char, L. Lee, S. Whiteley, and V. M. Hietala, "Superconducting Josephson arrays as tunable microwave sources operating at 77K," Appl. Phys. Lett., Sept. 1993.

[15] J. S. Martens, K. Char, A. Pance, L. P. Lee, M. E. Johansson, S. R. Whiteley, K. E. Kihlstrom, J. R. Wendt, V. M. Hietala, T. A. Plut, G. A. Vawter, S. Y. Hou, Julia M. Phillips, and W. Y. Lee, "The use of 2-dimensional arrays to determine the uniformity of Josephson junctions," IEEE Trans. on Appl. Superc. **3**, 3095 (1993).

3 Publications:

Two papers based on the work in this program have been published, these may included some work performed in a successor SBIR program be ;inning in July 1993 . They are references 3 and 4 above whose listing is repeated below.

J. S. Martens, A. Pance, K. Char, L. Lee, S. Whiteley, and V. M. Hietala, "Superconducting Josephson arrays as tunable microwave sources operating at 77K," Appl. Phys. Lett. **63**, 1681 (1993).

J. S. Martens, K. Char, A. Pance, L. P. Lee, M. E. Johansson, S. R. Whiteley, K. E. Kihlstrom, J. R. Wendt, V. M. Hietala, T. A. Plut, G. A. Vawter, S. Y. Hou, Julia M. Phillips, and W. Y. Lee, "The use of 2-dimensional arrays to determine the uniformity of Josephson junctions," IEEE Trans. on Appl. Superc. **3**, 3095 (1993).

<u>4 Personnel:</u>

Randy W. Simon

Current Position:

    Director of Research & Development and Vice-President of Marketing

Education:

    Ph.D., Physics, UCLA

    M.S., Physics, UCLA

    B.A., Physics, Pomona College

Experience:

    Randy Simon came to Conductus from TRW's Superconductivity Research Department where he headed up the high-temperature superconductivity program. Included in his responsibilities were the design and operation of thin film deposition systems, the investigation of Josephson device concepts, and the coordination of related programs in SQUIDs, microwave devices, and detectors. He also served as Principal Investigator on TRW's HTS DARPA project, and managed the Internal Research & Development Program on High-temperature Superconductive Electronics. He pioneered the use of lanthanum aluminate substrates for HTS films and developed several successful HTS Josephson device concepts. Before the HTS program, he was responsible for the development of TRW's niobium Josephson junction process and designed the dedicated deposition system used for the process. Prior to joining TRW, he conducted research on NbN films and tunnel junctions, and on granular composite films containing NbN. He also worked on the development of artificial tunneling barriers for all-refractory superconductor junctions. His graduate work at UCLA involved the fabrication of Josephson junctions using various barrier and multilayer techniques. Randy Simon brings expertise in both high- and low-temperature superconductor materials and devices and considerable project management experience to this program.

Jon Martens

Current Position:

Member of the Technical Staff

Education:

Ph.D., Electrical Engineering, University of Wisconsin

Experience:

Dr. Martens has a background in microwave/mm-wave circuit and device design and has been working on high speed superconducting electronics for the last 5 years. This includes work on Nb and HTS circuits at the University of Wisconsin and high speed HTS circuits at Sandia National Laboratories. The latter includes assisting in the development of two HTS junction technologies, the demonstration of HTS digital circuits, the development of the flux flow transistor to the stage of W-band amplification and the development of novel mm-wave materials characterization techniques. At Conductus he has worked on HTS digital and analog Josephson circuits (including a demonstration of HTS single flux quantum logic circuits), junction development and mm-wave measurements.

Aleksandar Pance

Current Position:

Member of the Technical Staff

Education:

Ph.D., Electrical Engineering, University of Rochester

Experience:

Aleksandar Pance joined Conductus after finishing his Ph.D. at the University of Rochester. His Ph.D. thesis deals with modeling, design, analysis and measurements of 2-D quasioptical Josephson junction arrays for 100 GHz-1 THz oscillators. He has performed microwave model measurements and characterization of 2-D active grid antenna arrays and numerical simulations of Josephson junction arrays in time domain. He has designed 2-D quasioptical arrays with 1000-1100 junctions for fabrication in Nb-based technology. He has proposed new Central frequency/Wideband design of quasioptical Josephson oscillator arrays with integrated tuning structures. Dr. Pance is currently involved in several projects dealing with both digital and analog high frequency applications of low and high temperature superconductors.

Kookrin Char

Current Position:

Manager, Device Development group

Education:

Ph.D., Applied Physics, Stanford University

M.S., Physics, UCLA

B. S., Physics, Seoul National University

Experience:

Kookrin Char has been responsible for thin film and device development based on pulsed laser deposition at Conductus since joining the company. He has designed and constructed a mullet-target laser deposition system whose target carousel has recently become a commercial product. He has developed processes for depositing state-of-the art YBCO films on buffered sapphire substrates. His multilayer technique has been successfully applied to produce engineered Josephson junctions in high-quality films. He leads the team that has developed the bi-epitaxial Josephson junction technology now in use at Conductus and is responsible for many of the key innovations behind Conductus' HTS JJ technology. Recently, he developed epitaxial HTS SNS Josephson junctions using $CaRuO_3$ as the metallic barrier. At Stanford University, he developed highly-successful mullet-source sputtering techniques for producing YBCO films and identified the existence of the "2-4-8" phase in these films. He also pioneered many techniques for processing YBCO films. Kookrin Char has maintained a position of leadership in high-temperature superconductor thin film materials and Josephson junctions since the earliest days of this new technology.

Marie Johansson

Current Position:

    Process Engineer

Education:

    Graduate courses (physics), University of Colorado, Boulder, 1990-1991

    Graduate courses (physics), University of Linkoeping, Sweden, 1988-1989

    BS, physics, University of Linkoeping, Sweden, 1986

Experience:

    Ms. Johansson gained experience in film-based x-ray tomography while at the University of Linkoeping. She spent three years in the development of passive microwave components while a researcher at the National Defence Research Institute in Linkoeping. During two years as a guest researcher in the Cryoelectronics Metrology Group of the NIST, Boulder, she gained extensive experience in the deposition and structural and electrical characterization of high temperature superconducting thin films as well as in the fabrication and electrical testing of devices made from these films. She joined Conductus in June 1992.

Stephen Whiteley

Current Position:

Manager, Digital Technologies group

Education:

Ph.D., Electrical Engineering and Computer Science, UC Berkeley

Experience:

Stephen Whiteley has an extensive background in superconductor and semiconductor circuit development. Most recently he has served as a consultant to several firms pursuing superconductive electronics development, particularly in the area of advanced signal processing components. He is currently developing an advanced Josephson circuit simulator based on SPICE3 as a commercial product. He served as the manager of the New Devices and Circuits Group at Hypres, Inc., where he designed complex Josephson circuitry that was often integrated with optical and other sensors. Upon completion of his doctorate, he worked for Tektronix, Inc. on designing a high-speed analog/digital bipolar LSI integrated circuit -- a time interpolator -- that is currently in use in the company's products. Stephen Whiteley's participation brings one of the foremost experts currently working in this field into the project.

5 Interactions:

Although the talk was not given during the term of this contract, it was based in part on the work described above:

"HTS Josephson arrays," 1993 International Superconducting Electronics Conference, Boulder, CO, 8/12-14/93.

6 New discoveries

A new quasi-3D topology with improved linewidth (discussed in section 2.3) was disclosed to the Air Force already. This novel structure capitalizes on the advantages of better current redirection to decrease the effects of critical current inhomogeneity on spectral linewidth.

7 Future thoughts

It is apparent that it is possible to extract radiation from YBCO Josephson arrays. The SNS junctions are attractive since their absolute parameters are in useful ranges and the spreads are not disastrous and are improving. It seems that some interesting subsystem requiring high microwave or mm-wave tunable sources would benefit substantially from this technology and its progeny. A follow-on program in progress should be able to answer the questions of where the technology can most improve and on what subsystems would benefit most from the pt. ormance available from these arrays.

AIR FORCE OF SCIENTIFIC RESEARCH (AFSC)
NOTICE OF TRANSMITTAL TO DTIC
This technical report has been reviewed and is
approved for public release IAW AFR 190-12
Distribution in unlimited.
Joan Buggs
STINFO Program Manager